DOI: 10.26345/EGRSE-007-17-202X

ANALYSIS OF SEISMIC WAVES AND ITS APPLICATION FOR PREDICTION OF IMPACTS ON BLASTING OPERATIONS IN THE QUARRY TREBEJOV ENVIRONMENT

ANALÝZA SEIZMICKÝCH VĹN A JEJ VYUŽITIE NA PREDIKCIU ÚČINKOV TRHACÍCH PRÁC V OKOLÍ LOMU TREBEJOV

Julián Kondela[1], Ján Baulovič[2], Blažej Pandula[3], Dušan Dugáček[4]

Abstract

The adverse or harmful seismic impact of the blasting operations is an important issue limiting the general and moreover reasonable tendency focused on the increase of the blasting operations extent. The unreasonable high technical seismic safety is the reason for the decrease of the explosive charges and blasting and as a consequence it causes the lower economic efficiency of both the shooting and blasting and quarrying. On the contrary, the underestimation of the seismic impacts could cause large scale material damages. Currently the identification of these harmful impacts and the assessment of the seismic security present an actual issue. In this paper there is described the method which enables due to the analysed data to assess the velocity of the seismic waves in the Trebejov quarry. The obtained data on the velocity of the seismic waves in the rock medium enable to optimize the millisecond timing of the blasting operations and therefore the attenuation of the seismic waves can be enlarged on the receptor and furthermore the seismic safety of the blasting operations can be ensured.

Abstrakt

Nežiaduci, či škodlivý seizmický účinok trhacích prác je dôležitý činiteľ, ktorý limituje všeobecnú a opodstatnenú tendenciu zväčšovať rozsah trhacích prác. Technicky neodôvodnená vysoká seizmická bezpečnosť vedie ku zmenšovaniu náloži a odstrelov, čím sa znižuje hospodárnosť rozpojovania a dobývania. Naopak, podcenenie seizmických účinkov môže spôsobiť veľké materiálne škody. V súčasnosti je identifikácia týchto škodlivých účinkov a stanovenie seizmickej bezpečnosti aktuálnym problémom. V článku je popísaná metóda, ktorá umožňuje na základe interpretovaných záznamov, stanoviť rýchlosť šírenia seizmických vĺn v lome Trebejov. Poznanie rýchlosti šírenia seizmických vĺn v horninovom prostredí lomu umožňuje optimalizáciu milisekundového časovania trhacích prác, a tak je možné zväčšiť útlm seizmických vĺn na receptore a zaistiť seizmickú bezpečnosť trhacích prác.

Keywords

blasting operations, Trebejov quarry, velocity of seismic waves, seismic safety, law of seismic waves attenuation

Kľúčové slová

trhacie práce, lom Trebejov, rýchlosť seizmických vĺn, seizmická bezpečnosť, zákon útlmu seizmických vĺn

1 Introduction

The compression force, which arises in the place of the explosion, generates stress waves in the neighbouring elastic medium. These waves propagate into the surrounding area and carry forward the energy of the explosion along further distances. The stress waves carry on the stress to the surrounding rock medium. Near to the seismic source and in the distance of some few meters the generated stress proves the characteristics of a compression wave. The compression force increases up to a maximum value and then it begins to fall gradually to the value of zero. There can be observed the attenuated vibration of the medium. According to the increasing distance from the seismic source both the stress form and the generated movement of the transmitting medium change. After a sudden fall of the pressure its decrease does not end at the value of zero but the first part of the excess pressure is followed by the further second region of the under pressure of the propagating wave. The medium deformation is characterized by the vibration. In each elastic medium of the solid state the arising of the longitudinal stress P-wave is followed by a transverse S-wave. It originates at the transmission and reflection of the longitudinal wave at the interface of various media. [1], [2], [4], [5], [7], [8], [9], [12], [13], [15], [16], [18]

The velocity P-waves is as follows[1],[2],[7],[8], [9], [12], [13], [18]:

$$c_p = \sqrt{\frac{K + \frac{4}{3} \times G}{\rho}} = \sqrt{\frac{E \times (1 - \mu)}{\rho \times (1 - 2\mu) \times (1 + \mu)}} \text{ in [m/s],} \qquad (1)$$

where

K – is the modulus of the bulk elasticity of the medium [kg×m^{-1}×s^{-2}],

G –is the shear modulus [kg×m^{-1}×s^{-2}],

ρ – is the bulk density of the medium [kg×m^{-3}],

E – is the Young´s modulus of elasticity [kg×m^{-1}×s^{-2}] and

μ – is the Poisson´s ratio [-].

The velocity of the S-waves can be expressed by the following relation[1],[2],[7],[8], [9], [12], [13], [18]:

$$c_s = c_p \times \sqrt{\frac{1 - 2\mu}{2 \times (1 - \mu)}} \text{ in [m/s].} \qquad (2)$$

In S-wave the particle displacement is perpendicular to the direction of wave propagation. The particles oscillate like a violin string and the periodically growing stress changes. Those waves cannot be formed in a liquid or gas but entirely in a solid material. From the equations for P-waves and S-waves it follows that $c_p/c_s \geq \sqrt{2}$ and that $c_p \geq 1.4\ c_s$. The velocity S-waves is therefore about half as small as the velocity of the P-waves so that they come to a certain point later; see fig.1.

The bulk waves spread out longitudinally and transversely into the whole medium. Their intensity quickly decreases in relation to the distance. If the environment is limited by the surface, which is always the case, other types of waves are formed by interaction of the transverse and longitudinal waves. These waves spread only near the surface and are called surface waves. Depending on the nature of their propagation, we can recognize Rayleigh's R-waves and the Love L-waves. Because they propagate relatively in a narrow band adjacent to the surface, their energy decreases more slowly than with volumetric waves. R-waves indicate the soil's particles into elliptical motion, much like the water particles waving its surface. Their velocity can be expressed like this: $c_{\mathbf{R}} = \mathbf{0{,}92} \times c_{\mathbf{S}}$.

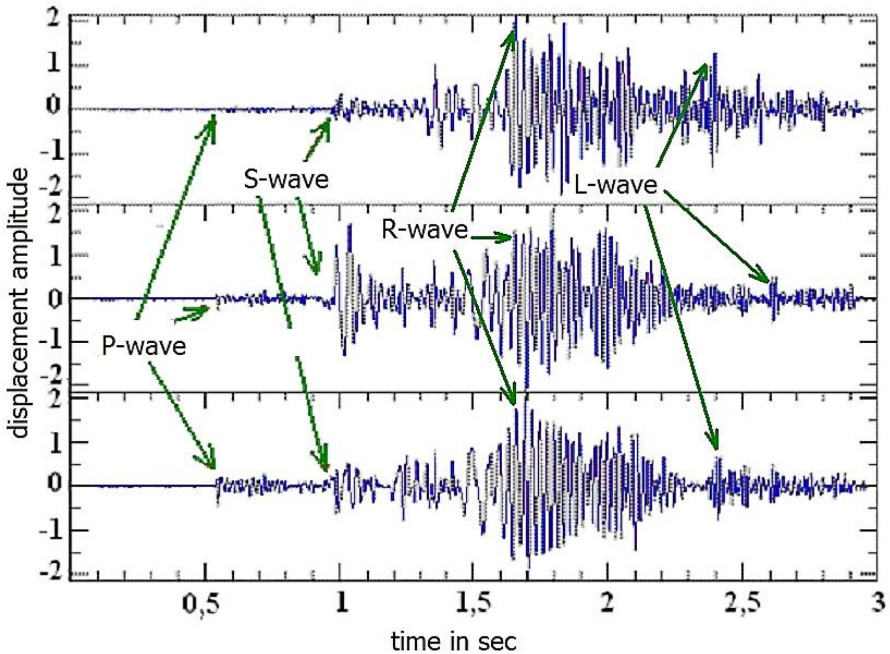

Fig. 1 Examples of seismic records capturing the arrival of P-waves, S-waves,R-waves and L-waves

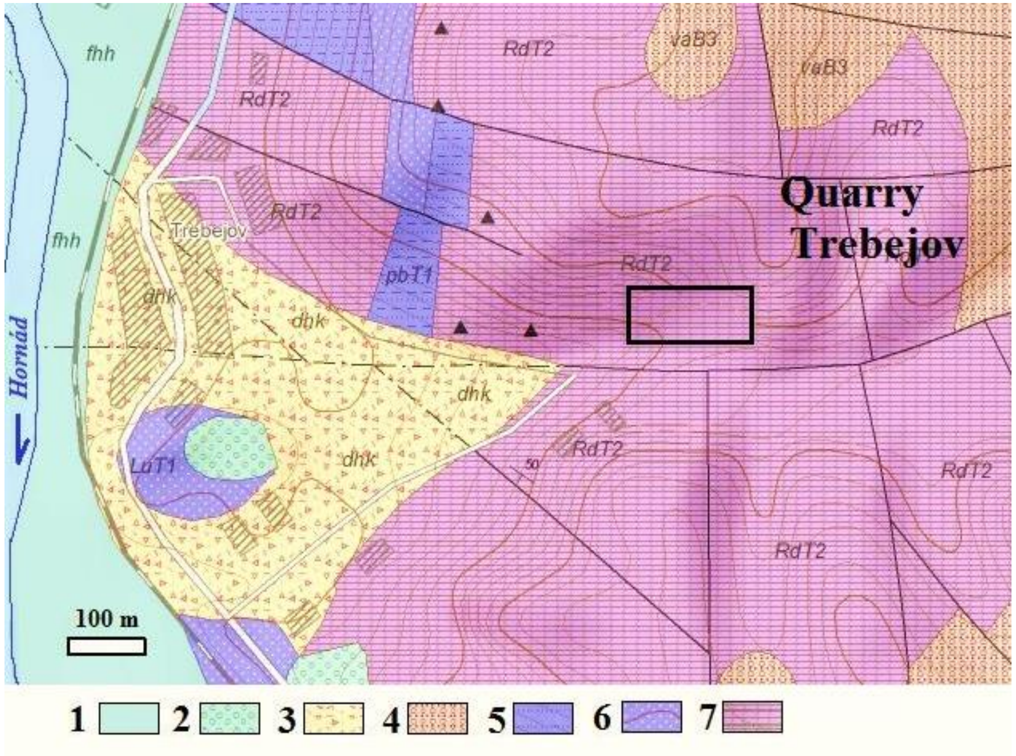

Fig. 2 Geological map of the surroundings of the quarry Trebejov

Explanations to Fig. 2: *Quaternary*: 1 – clay, gravel, sand (Holocene), 2 – sandy gravel, gravel (Pleistocene), 3 – deluvium (unstructured) mainly loam stony, *Neogene*: 4 – klčovské formation varhaňovské gravel: polymict, weathered, without pebbles of carbonates (upper Baden-lower Sarmatian), *Mesozoic*: 5 – variegated clayey shales, clay sandy shales, with interbeds of quartzite (lower Trias), 6 – lúžňanské formation– quartzite, quartzite sandstone, locally with the interbed shales (lower Trias), 7 – Ramsau dolomites (ladin). More is in Geological map of the Branisko and Čierna Hora. [17]

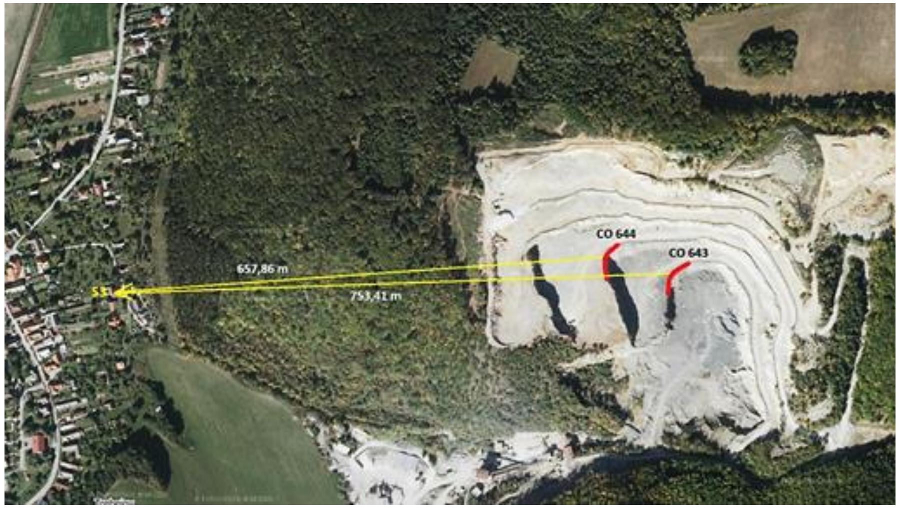

Fig.3 Position and distance of measurement standpoint S3 from bench blasts CO 643 and from CO 644

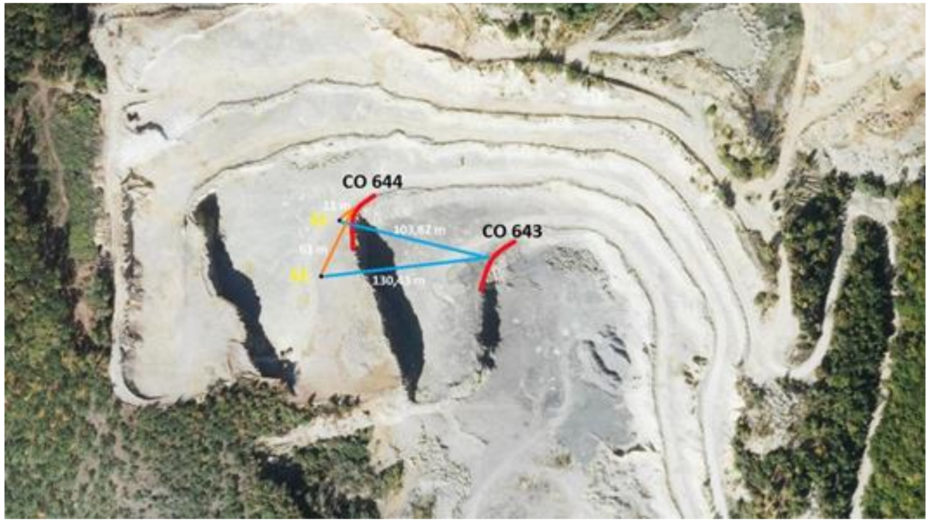

Fig.4 Position and distance of measurement standpoints S1 and from bench blast CO 643 and from bench blast CO 644

Another type of surface waves is L-waves. Transmission environments in it perform a horizontal movement perpendicular to the wave propagation direction, as in S-waves, but their intensity decreases with the distance from the surface.[2],[3], [4],[5],[7] ,[8], [9], [10], [11], [12], [13], [15], [16],[18]

At very close distances from the source, all waves are due to very small differences in their velocities in one waveform. At a sufficiently large distance, two waves of P-wave and S-wave can be precisely separated. In the case of blasting, it is at a distance of more than 150m radius of charge.[12],[13],[15], [16]

2 Experimental measurements in the Trebejov quarr

The quarry Trebejov is situated 13.0 km north from Košice, in the land registry of the village Trebejov. The quarry Trebejov is situated 700 m east from the given village. Region is integrated into the mountains Čierna Hora (254 km^2), which is west and south-west neighbouring with Volovské Vrchy, in a shorter distance on the north-west with the Hornád basin and Branisko – the south it is separated from the Šarišská vrchovina by troughs, on the east it gradually continues to the Košice basin. The studied region has a complicated geological structure. In the middle part of the mountain there prevail the rocks of crystalline on which the less fragmented plain relief can be found. The northern and southern borders of the mountain are created from the residuals of the Mesozoic nappes (limestone and dolomite), on which the more fragmented forms of the relief developed. The geological structure of the deposit and its wider surroundings are complex and the petrography is dissimilar. Different types of limestones and predominate Ramsau dolomite of Triassic age; see fig. 2.[14]

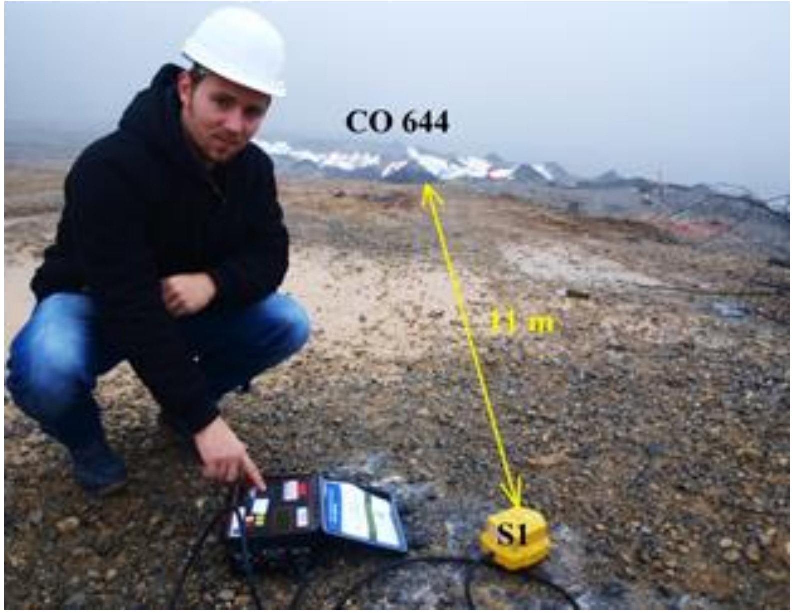

Fig. 5 Position of the seismograph VMS 2000 MP, standpoint S1 at a distance of 103.9 m from the first bench blast CO 643 and at distance of 11 m from the second bench blast CO 644 in quarry Trebejov

Fig. 6 Position of the seismographs UVS 1504 and ABEM Vibraloc, standpoint S3 (residential building) at a distance of 753.4 m; the first bench blasting CO 643 and at a distance of 657.9 m from the second bench blasting CO 644 in the village Trebejov

3 Measuring standpoints and the types of applied apparatuses at measuring

The sources of the seismic effects were the monitored bench blasts CO 643 and CO 644 at the deposit of dolomites located approximately 0.7 km east from the village Trebejov, see fig.3 and fig.4. [14] To measure and graphically record the seismic effects of the bench blasts in the quarry Trebejov the following digital seismic apparatuses were applied:

- seismograph VMS 2000 MP of the American company Thomas Instruments and seismic recorders of the American company Geospace; fig. 5.
- seismograph ABEM Vibraloc and seismic recorders of the Swedish company ABEM; fig. 6.
- seismograph UVS 1504 and seismic recorders of the Swedish company Nitro Consult; fig. 6.

Tab. 1 Data about the blast positions and distance of the standpoints in the Trebejov quarry

Standpoint	**Blast**	**Distance from blast to the standpoint [m]**		**Note**
		Diagonal [m]	**Horizontal [m]**	
S1	CO 643	106.6	103.8	quarry
S2	CO 643	132.6	130.4	quarry
S3	CO 643	753.8	753.4	village
S1	CO 644	26.4	11.0	quarry
S2	CO 644	65.6	61.0	quarry
S3	CO 644	658.3	657.9	village

- At measuring the seismic effects of the bench blasting at the standpoint S1, fig. 5, the seismograph VMS 2000 MP was applied.
- The measuring of the seismic effects at the standpoint S2 was carried out by the digital four-channel seismograph Vibraloc and by seismic recorders of the Swedish company ABEM. The measuring standpoint S3 was set on the concrete basis at the entrance of the examined object – a family house in the village Trebejov. At measuring the seismographs UVS 1504 and Vibraloc were applied; see fig. 6.
- The bench blasts No. 643 (hereafter only as CO 643) and bench blast No. 644 (hereafter only as CO 644) in the Trebejov quarry were the source of the seismic effects. The blasts were situated in the quarry as depicted in fig. 3 and fig. 4. According to the registered records the following part of this investigation will be the analysis of the seismic waves generated by the blasting operations and consequently the assessment of the velocity waves in the rock medium.

At the CO 643, which was carried out at the first stage, there were drilled 21 vertical boreholes, in total 467.2 m. The boreholes were drilled at average of 105 mm. The total length of the borehole sealing was 76.0 m. For the ignition the following explosives were applied: Ecodanubit – 157.5 kg, Infernit – 50.0 kg and Austinit – 2860.0 kg. The total explosive charge in the boreholes was 3067.5 kg. For the non-electric ignition the following material was used – 41 pc of Indetshock MS 20/50. At the CO 644, which was carried out at the second stage, there were drilled 30 vertical boreholes, in total 863.0 m. The average of the boreholes was 105 mm. The total length of the borehole sealing was 105.0 m. For the ignition the following explosives were used Ecodanubit – 225.0 kg, Infernit – 75.0 kg, Austinit – 2280.0 kg, DAP E – 1500.0 kg and DAP 2 – 1325.0 kg. The total explosive charge in the boreholes was 5405.0 kg. For the non-electric ignition the following material was used – 60 pc of Indetshock MS 20/50. Distance from blast to the stand points as follows in tab.1.

4 The measured seismic effects of the bench blasting and their analysis

The apparats placed at the particular measuring standpoints were gauged before the measurements and their responsiveness was assessed. At the measuring standpoints the graphical responses of individual parts of the seismic vibration were recorded at CO 643 and CO 644. The individual graphical records were four seconds. The seismic measuring apparats were set at the measuring standpoints in order to evaluate the impact of the generated technical seismicity. The measured values of the seismic effects generated by the bench blasting in the Trebejov quarry are depicted in tab.2 and tab.3.

Tab. 2 Measured values of the frequency and particle velocity at CO 643

CO 643 – I. stage	X [Hz]	Y [Hz]	Z [Hz]	X [mm×s^{-1}]	Y [mm×s^{-1}]	Z [mm×s^{-1}]
Standpoint S1 – Trebejov quarry	23.30	13.80	26.9	32.140	37.220	48.150
Standpoint S2 – Trebejov quarry	27.10	12.10	33.5	13.559	9.710	11.603
Standpoint S3 – family house in the village Trebejov	6.29	9.19	23.8	1.304	1.418	0.809

Tab. 3 Measured values of the frequency and particle velocity at CO 644

CO 644 – II. stage	X [Hz]	Y [Hz]	Z [Hz]	X [mm×s^{-1}]	Y [mm×s^{-1}]	Z [mm×s^{-1}]
Standpoint S1 – Trebejov quarry	17.10	23.3	23.3	91.440	102.370	135.060
Standpoint S2 – Trebejov quarry	17.10	18.8	40.3	23.167	16.922	32.370
Standpoint S3 – family house in the village Trebejov	8.86	15.2	12.8	1.536	0.926	1.156

Our investigation was focused on the detailed analysis of the seismic waves generated by the first and the second blasts and they were recorded at the measuring standpoints S2 and S3. These measuring standpoints were in different distances from the source and it enabled us, according to various arrival times of the seismic waves, to assess the propagation speed in the Trebejov quarry as well as to the residential objects in the village Trebejov. [14]

At the measuring standpoint S1 at CO 643 the wave's propagation was as follows in fig.7:

- **vibration component – X:** at the time 58 ms after the arrival of the P-wave, the arrival / entry of S-wave was recorded. At the time 216 ms was recorded arrival/entry the R-wave. The wave propagation continued and at the time 327 ms was recorded arrival/entry the L-wave and the L wave´s vibration did not stabilize either at the time 2000 ms,
- **vibration component – Y**: at the time 51 ms after the arrival of the P-wave, the arrival / entry of S-wave was recorded. At the time 117 ms was recorded arrival/entry the R-wave. The wave propagation continued and at the time 367 ms was recorded arrival/entry the L-wave and the L wave´s vibration did not stabilize either at the time 2000 ms,

- **vibration component – Z:**at the time 51 ms after the arrival of the P-wave, the arrival / entry of S-wave was recorded. At the time 213 ms was recorded arrival/entry the R-wave. The wave propagation continued and at the time 334 ms was recorded arrival/entry the L-wave and the further propagation continued up to the time 856 ms.

At the measuring standpoint S1 during the second bench blast CO 644 the waves behaved in different types of the vibration components as follows; fig.8:

- vibration component – X: at the time 22 ms after the arrival of the P-wave, the arrival/entry of S-wave was recorded. At the time 66 ms was recorded arrival/entry the R-wave. The wave propagation continued and at the time 158 ms was recorded arrival/entry the L-wave and the L wave´s vibration did not stabilize either at the time 2000 ms,
- vibration component – Y: after the termination of the P-wave at the time 18 ms the S-wave arrived which lasted up to the time 69 ms. The vibration did not stabilize and it continued by the arrival of the R-wave which terminated at the time 169 ms and the next wave was L-wave which did not terminate its vibration either at the time 2000 ms,
- vibration component – Z: at the time 14 ms after the arrival of the P-wave, the arrival/entry of S-wave was recorded. At the time 73 ms was recorded arrival/entry the R-wave. The wave propagation continued and at the time 172 ms was recorded arrival/entry the L-wave and the L wave´s vibration did not stabilize either at the time 2000 ms.

The vibration arrived in 51 ms at the first measuring standpoint which was 106.6 m far from the CO 643 (slant distance at the depth 24 m, in which the initiating charge was placed in the borehole). The measuring standpoint S1 which

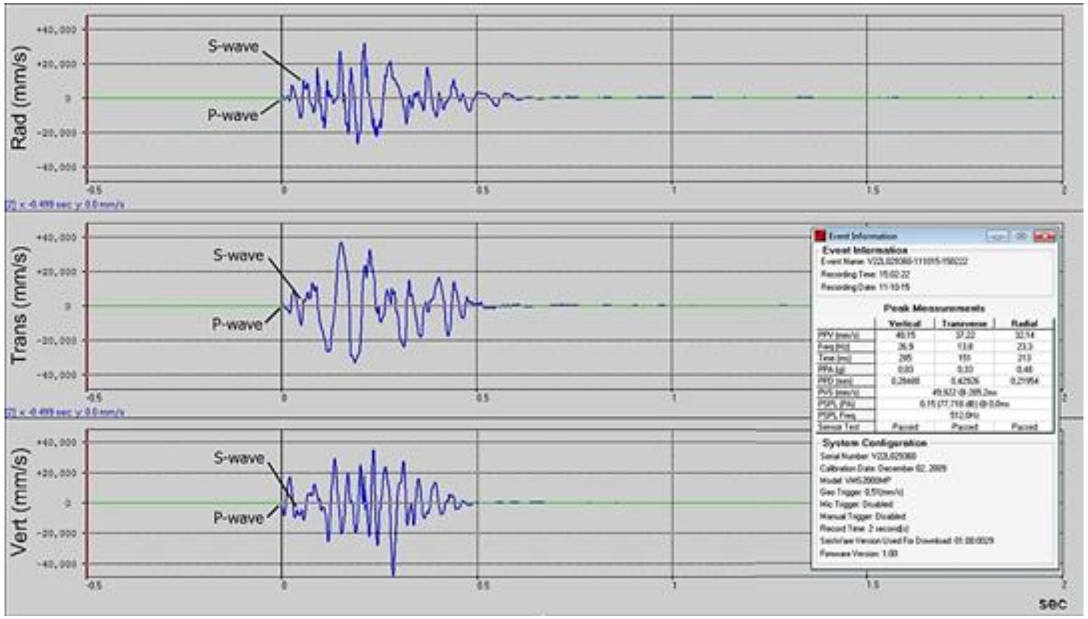

Fig. 7 Waves arrive at standpoint S1 at CO 643

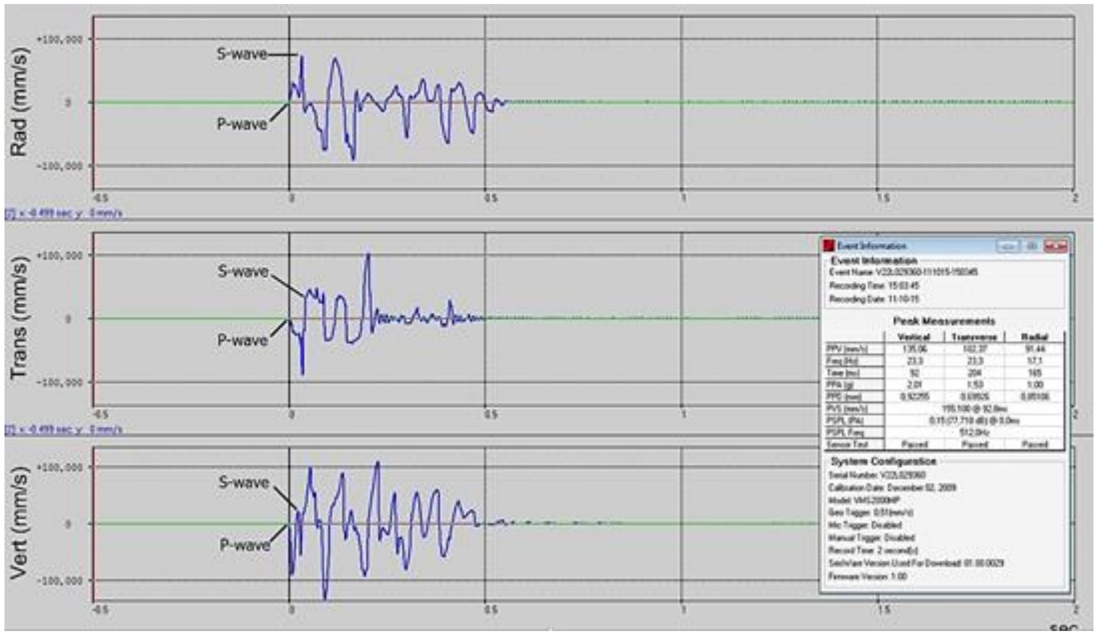

Fig. 8 Waves arrive at standpoint S1 at CO 644

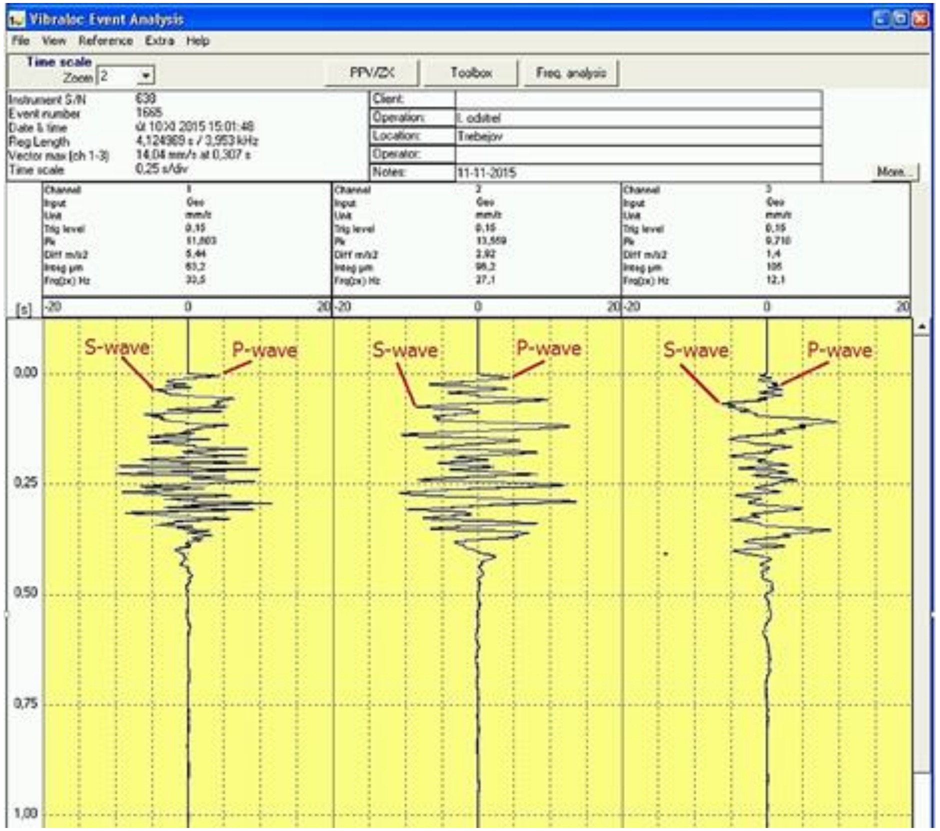

Fig. 9 Waves arrive at standpoint S2 at CO 643

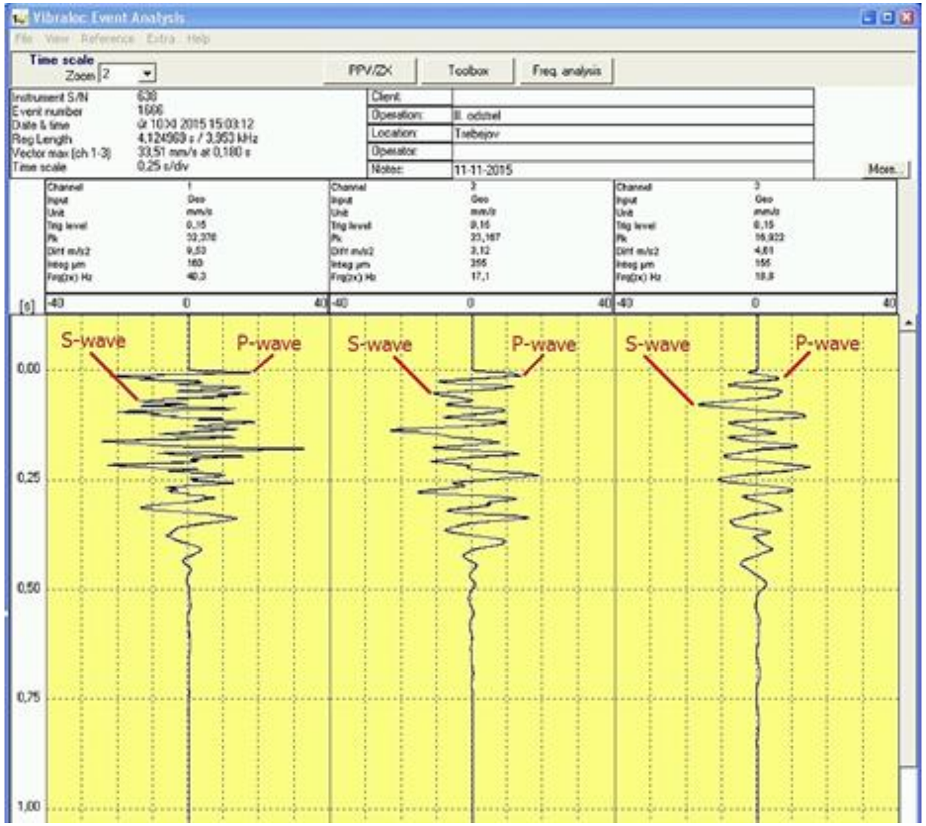

Fig. 10 Waves arrive at standpoint S2 at CO 644

was 26.4 m far from the second CO 644 also recorded the vibration (slant distance at the depth 24 m, in which the initiating charge was placed in the borehole). The vibration from the second blast arrived at the measuring standpoint in 18 ms. According to these data we were able to assess the approximate velocity S-wave at the measuring standpoint S1, which was 2430 $m \times s^{-1}$.

At the measuring standpoint S2 at the CO 643 the waves behaved in different types of the vibration components as follows in fig.9:

- the first channel – Z: at the time 19 ms after the arrival of the P-wave, the arrival/entry of S-wave was recorded. At the time 142 ms was recorded arrival / entry the R-wave. The wave propagation continued and at the time 262 ms was recorded arrival/entry the L-wave and the L wave´s vibration did not stabilize either at the time 1402 ms,
- the second channel – X: at the time 49 ms after the arrival of the P-wave, the arrival / entry of S-wave was recorded. At the time 84 ms was recorded arrival / entry the R-wave. The wave propagation continued and at the time 275 ms was recorded arrival / entry the L-wave and its vibration carried on and did not stabilize either at the time 2000 ms,

- the third channel – Y: at the time 30 ms after the arrival of the P-wave, the arrival/entry of S-wave was recorded. At the time 97 ms was recorded arrival/entry the R-wave. The wave propagation continued and at the time 217 ms was recorded arrival/entry the L-wave and its vibration carried on and did not stabilize either at the time 2000 ms.

At the measuring standpoint S2 during the second blast the waves behaved in different types of the vibration components as follows in fig.10:

- the first channel – Z: at the time 31 ms after the arrival of the P-wave, the arrival/entry of S-wave was recorded. At the time 81 ms was recorded arrival/entry the R-wave. The wave propagation continued and at the time 223 ms was recorded arrival/entry the L-wave and it vibrated further up to the time 782 ms,
- the second channel – X: at the time 23 ms after the arrival of the P-wave, the arrival/entry of S-wave was recorded. At the time 77 ms was recorded arrival/entry the R-wave. The wave propagation continued and at the time 247 ms was recorded arrival/entry the L-wave and it vibrated further up to the time 2000 ms,
- the third channel – Y: at the time 31 ms after the arrival of the P-wave, the arrival / entry of S-wave was recorded. At the time 123 ms was recorded arrival/entry the R-wave. The wave propagation continued and at the time 272 ms was recorded arrival/entry the L-wave and it vibrated further up to the time 2000 ms.

The vibration arrived in 49 ms at the second measuring standpoint, which was 132.6 m far from the CO 643 (slant distance at the depth 24 m, in which the initiating charge was placed in the borehole). The measuring standpoint S2 which was 65.6 m far from the second CO 644 also recorded the vibration (slant distance at the depth 24 m, in which the initiating charge was placed in the borehole). The vibration from the second blast arrived at the measuring standpoint in 23 ms. According to these data we were able to assess the approximate velocity S-wave at the measuring standpoint S2, which was 2570 $m \times s^{-1}$.

At the measuring standpoint S3 at the CO 643 the waves behaved in different types of the vibration components as follows in fig.11:

- the first channel – Z: at the time 227 ms after the arrival of the P-wave, the arrival/entry of S-wave was recorded. At the time 396 ms was recorded arrival/entry the R-wave. The wave propagation continued and at the time 577 ms was recorded arrival/entry the L-wave and it vibrated further up to the time 4000 ms,
- the second channel – X: at the time 220 ms after the arrival of the P-wave, the arrival/entry of S-wave was recorded. At the time 402 ms was recorded arrival/entry the R-wave. The wave propagation continued and at the time 584 ms was recorded arrival/entry the L-wave and it vibrated further up to the time 4000 ms,
- the third channel – Y: at the time 292 ms after the arrival of the P-wave, the arrival/entry of S-wave was recorded. At the time 409 ms was recorded arrival/entry the R-wave. The wave propagation continued and at the time 629 ms was recorded arrival/entry the L-wave and it vibrated further up to the time 4000 ms.

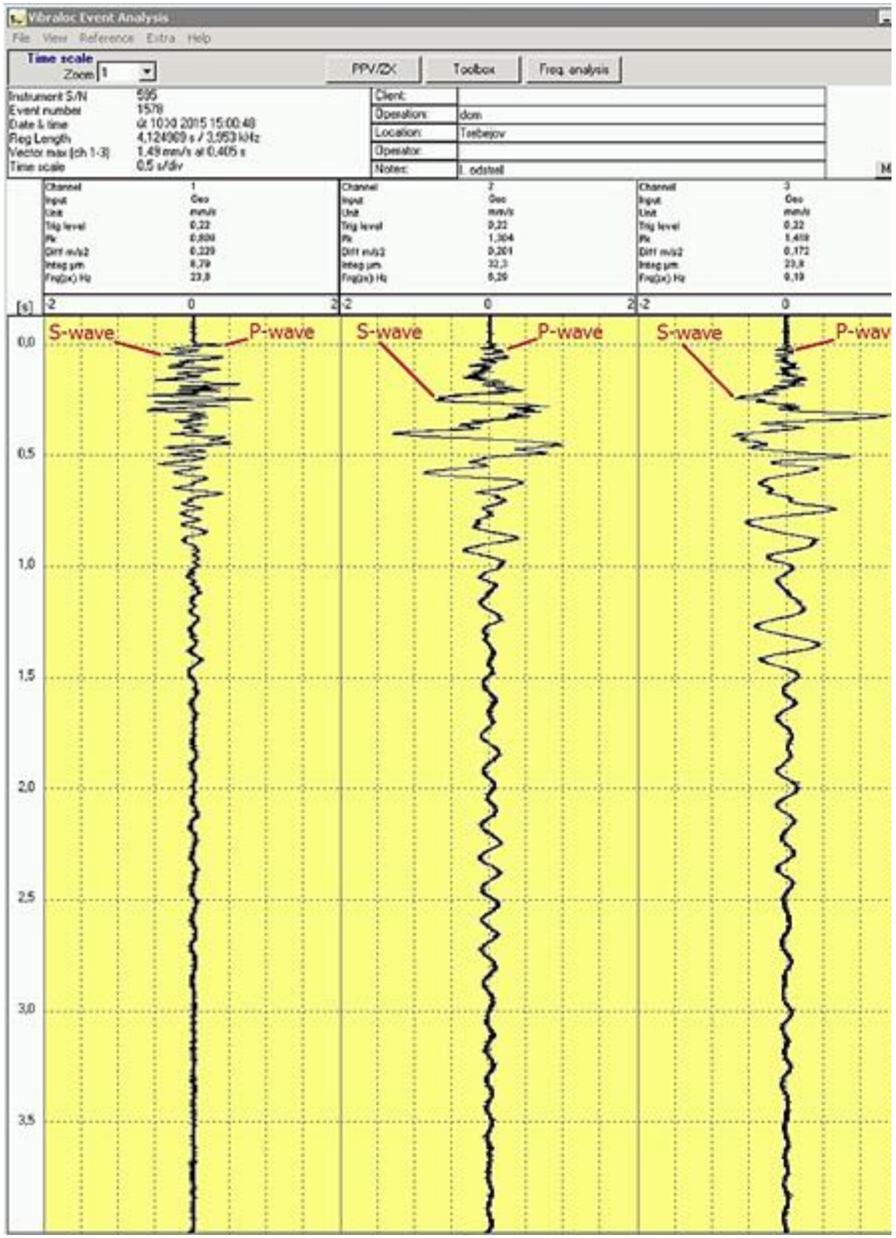

Fig. 11 waves arrive at standpoint S3 at CO 643

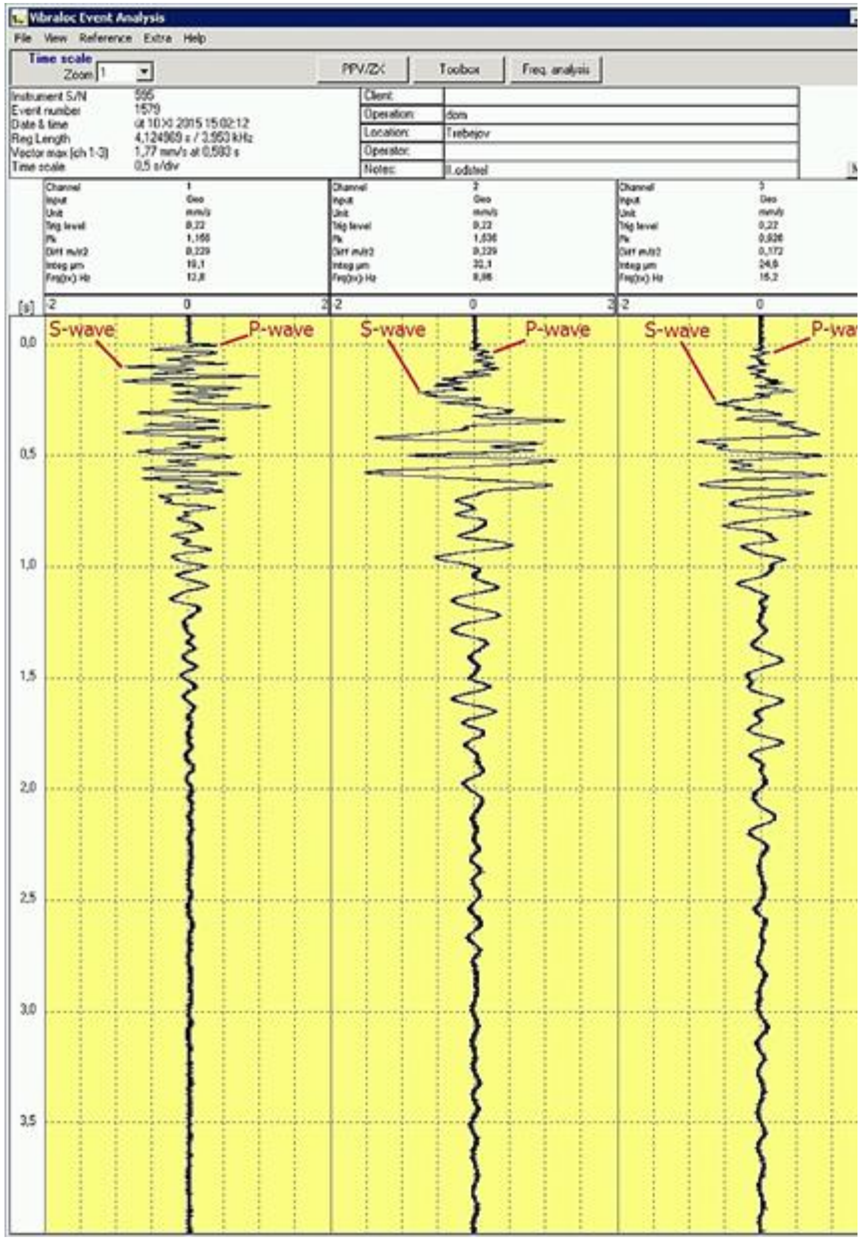

Fig. 12 waves arrive at standpoint S3 at CO 644

At the measuring standpoint S3 at the CO 644 the waves behaved in different types of the vibration components as follows in fig.12:

- the first channel – Z: at the time 253 ms after the arrival of the P-wave, the arrival/entry of S-wave was recorded. At the time 448 ms was recorded arrival/entry the R-wave. The wave propagation continued and at the time 694 ms was recorded arrival/entry the L-wave and it vibrated further up to the time 4000 ms,
- the second channel – X: at the time 305 ms after the arrival of the P-wave, the arrival/entry of S-wave was recorded. At the time 415 ms was recorded arrival/entry the R-wave. The wave propagation continued and at the time 577 ms was recorded arrival/entry the L-wave and it vibrated further up to the time 4000 ms,
- the third channel – Y: at the time 227 ms after the arrival of the P-wave, the arrival/entry of S-wave was recorded. At the time 435 ms was recorded arrival/entry the R-wave. The wave propagation continued and at the time 558 ms was recorded arrival/entry the L-wave and it vibrated further up to the time 4000 ms.

The vibration arrived in 292 ms at the third measuring standpoint, which was 753.8 m far from the CO 643 (slant distance at the depth 24 m, in which the initiating charge was placed). The measuring standpoint S3 also recorded vibration from the CO 644, which was in the distance 658.3 m (slant distance). The vibration from the second blast arrived at the measuring standpoint in 305 ms. In order to determine the seismic wave's arrival time it is necessary to take into consideration also the measuring standpoint S2. The wave arrived in 30 s at the measuring standpoint S2, which was 132.6 m far from the CO 643 (slant distance). The waves from the CO 644, in the distance of 65.6 m (slant distance) also arrived at this measuring standpoint. The vibration arrived in 23 ms. According to these data we were able to assess the approximate velocity S-wave at the measuring standpoint S3, which has registered 2370 $m \times s^{-1}$ in case of the CO 643 and it was 2100 $m \times s^{-1}$ in case of the CO 644.

According to the measured and calculated data it can be stated that the average velocity seismic S-waves in the Trebejov quarry at the first and the second stages, where the blasting operations were carried out, were from 2430 up to 2570 $m \times s^{-1}$, which correspond to a slightly disturbed rock medium from the viewpoint of the seismic wave's propagation. The approximate seismic wave's velocity between the source of the seismic waves and the receptor, in our case it was a family house in the village Trebejov, was from 2100 $m \times s^{-1}$ up to 2370 $m \times s^{-1}$.

The comparison of the above given data confirms that the receptor is at the rock massive, in which the blasting operations were carried out. This is the reason for the recorded long lasting vibrations up to 4000 ms at this receptor. Taking into consideration the seismic safety of the blasting operations it presents an important factor because the dwellers of the housing objects can consider the vibrations to be dangerous for them. In the process of blast design it is highly required to take into account this factor.

5 Conclusions

The aim of this research was to identify the different types of the seismic waves generated in the blasting operations and moreover to analyse them. According to our analysis we assessed the arrival times of the S-waves, R-waves and L-waves at the various measuring standpoints. According to the different distances and arrival times of the seismic waves at the particular measuring standpoints S1, S2 and S3 the velocity of the seismic S-waves was determined in the Trebejov quarry and moreover to the receptor which was the family house in the village Trebejov. This residential object was selected for the monitoring as for a long time the dwellers complained about the vibration generated in the blasting operations in the Trebejov quarry.

The important issue was the assessment of the particular value of the velocity of the seismic waves between the receptor and the source of the vibration. According to this value the maximum value of the seismic waves attenuation can be determined by applying an appropriate millisecond timing and consequently to secure the maximum seismic safety of the residential objects in the village Trebejov. To meet this requirement is the main goal of the blasting operations design. Furthermore the values of the velocity of the seismic waves in the rock medium, in which the blasting operations are carried out, are very important in the process of the blasting operations design. Due to the values of the velocity of the seismic waves in the rock medium, in which the blasting operations are carried out, there can be determined the number of boreholes and the charge capacity required for the rock disturbance and finally it can lead to economic efficiency of the blasting operations.

In terms of the assessed values of the velocity of the seismic S-waves it enables us to optimize the millisecond timing of the blasting operations in order to secure the highest possible attenuation of the seismic effects, generated during the blasting operations, from the blast to the receptor. In this way the seismic safety of the blasting operations can be improved and furthermore the undesirable effect on the neighbouring environment can be reduced.

References

[1] AKI, K., RICHARDS, P. G. *Quantitative Seismology*, Theory and Methods, San Francisco, 1980, 933 p.

[2] BARTON, N. *Rock quality. Seismic velocity. Attenuation and Anisotropy.* London, 2007, 721 p.

[3] BLAHA, I., MŮLLER, K. Application of Geophysical Methods, Geotechnics and Construction, In: *International Journal of Exploration Geophysics (EGRSE),* Vol. 10, No. 1-2, 2003, p. 20-24.

[4] BOLIČEVSKIJ, J. M. *Sposob rasčeta skorostej uprugich voln v anizotropnych treščinnych gornych porodach*, Saratov, 1983, 183 p.

[5] HENRYCH, J. *Dynamics of explosion and its use*, Praha, 1973, 210 p.

[6] CHEN, C. H. *Seismic Signal Analysis and Discrimination,* Amsterdam-Oxford-New York, 1982, 102 p.

[7] DOJČÁR, O., HORKÝ, J., KOŘÍNEK, R, *Blasting techniques*, Ostrava, 1996. 256 p.

[8] DVOŘÁK, A. *Fundamentals of seismic technique*, Praha, 1969, 128 p.

[9] KALAB, Z. *Seismic measurement in geotechnics,* Ostrava 2008, 124 p.

[10]KALAB, Z., KNEJZLIK, J.,LEDNICKÁ, M., DOLEŽALOVÁ, H., HRUBEŠOVÁ, E. *Study of Seismic Impact in Surroundings of Seismic Station Depending on Local Geological Conditions*, Montanex, Ostrava, 2010, 126 p.

[11KALÁB, Z., PANDULA, B., STOLÁRIK, M., KONDELA, J. Examples of law of seismic wave attenuation, *Metalurgija*, Vol. 52, Issue 3, 2013, p. 387-390.

[12] MOSINEC, V. N. *Drobjaščeje i sejsmičeskoje dejstvija vzryva v gornych porodach*, Moskva, 1976, 187 p.

[13] PANDULA, B., KONDELA, J.*Methodology of seismic blasting*, Banská Bystrica, 2010,156 p.

[14]PANDULA, B., KONDELA, J. *Measurement of the impact of technical seismicity in Trebejov quarry on the surrounding area of Trebejov village*, Research Report F BERG TU Košice, 2016, 27 p.

[15] PANDULA, B., KONDELA, J., HOLUB, K. Investigation on seismic signals for blasting in quarries, In*: EGRSE*, Vol. 19, no. 1, 2012, p. 41-59.
[16] PANDULA, B. KONDELA, J., FRIEDMANNOVÁ, M. Research of technical seismicity in the Maglovec quarry, in*: EGRSE*, Vol. 22, no. 2, 2013, p. 14-29.
[17]JACKO, S.,., POLÁK, M.., VOZÁR, J., VOZÁROVÁ, A., GROSS, P., HARČÁR, J., SASVÁRI, T., ZACHAROV, M., BALÁŽ, B., KALIČIAK, M., KAROLI, S., NAGY, A., BUČEK, S., MAGLAY, J., SPIŠÁK, Z., ŽEC, B., FILO, I., JANOČKO, J. *Geological map of the Branisko and Čierna Hora Mts.*, GSSR - Bratislava, 1996.
[18] TOWHATA, I. *Geotechnical earthquake engineering*, Springer, 2008, 684 p.

Authors
[1] Doc. Julián Kondela, PhD., Ústav Geovied Fakulta BERG TU v Košiciach, Park Komenského 15, 043 84 Košice, Julian.Kondela@tuke.sk
[2] Ing. Ján Baulovič, bblast s.r.o., Jasenov 282, 06601 Humenné, Slovensko, jbaulovic@centrum.sk
[3]Prof. RNDr. Blažej Pandula, CSc., Ústav Geovied Fakulta BERG TU v Košiciach, Park Komenského 19, 043 84 Košice, Blazej.Pandula@tuke.sk
[4]Ing. Dušan Dugáček, PhD., Ústav Geovied Fakulta BERG TU v Košiciach, Park Komenského 15, 043 84 Košice, Dusan.Dugacek@tuke.sk